Materials and Design 30 (2009) 330–334

Contents lists available at ScienceDirect

Materials and Design

journal homepage: www.elsevier.com/locate/matdes

Design of a multi-hole extrusion process

M.K. Sinha, S. Deb, U.S. Dixit *

Department of Mechanical Engineering, Indian Institute of Technology Guwahati, Guwahati 781 039, India

ARTICLE INFO

Article history:
Received 30 November 2007
Accepted 26 April 2008
Available online 3 May 2008

Keyword:
C. Extrusion

ABSTRACT

This work describes the procedure for the design of a multi-hole extrusion process. For the same sizes of the holes, the ram force in a single-hole extrusion process is more than in a multi-hole extrusion process. Therefore, a simplified upper bound and slab method analysis has been carried out for a single-hole extrusion process. The ram and die pressures obtained from this analysis are used for designing a multi-hole extrusion process setup. The stresses in the die are computed using the finite element method. Based on this approach, an experimental setup was fabricated and experimental study was carried out.

1. Introduction

Multi-hole extrusion is the process in which the raw material is pushed through a die having more than one hole. This process is highly productive for producing parts of smaller length and cross-section. For the given billet and final product size, the requirement of the ram force is lesser in the multi-hole extrusion than in the single-hole extrusion. The process has great importance for producing micron-size parts.

For the design of a multi-hole die extrusion machine, the modeling of the extrusion process is required. Although the finite element method can be effectively employed for this purpose [1–8], it requires a large amount of computational time besides the requirement of appropriate software to do the mesh generation and finite element processing. After the tentative or final specifications are decided, the design process usually consists of three stages: the conceptual design, the embodiment or preliminary design and the detailed design. At the conceptual design stage, the design concepts are generated. At the preliminary design stage, the chosen concept is given bodily form. Finally, at the detailed design stage, the detailed design calculations are carried out and the manufacturing drawings are generated. At the preliminary design stage, one needs computationally faster analysis for generating an optimum design. The generated design at this stage can be further fine tuned with rigorous finite element analysis of the process.

In view of this, this article presents a simplified procedure for carrying out the necessary design calculations for the design of the extrusion process. The methodology makes use of the upper bound method, the slab method and the linear-elastic finite element analysis. The proposed method is validated by experiments.

The research on multi-hole extrusion is several decades old. A brief review of the related work is as follows. Dodeja and Johnson [9] carried out experiments to cold extrude pure lead, tellurium lead, pure tin and super pure aluminium through square dies containing up to four holes arranged in different patterns. They provided empirical expressions for the calculation of the ram force. Slip-line fields have been proposed for the analysis of the process [10], although they are limited to plane-strain extrusion of non-hardening materials. Keife [11] has carried out two-dimensional upper bound analysis of extrusion through two die openings. The validation was carried out by extruding plasticine. Xie et al. [12] have investigated the flow behavior of metal in the extrusion of a pipe into a porthole-die. They have employed a kind of visioplasticity method. Ulysee and Johnson [13] have presented analytical and semi-analytical upper bound solutions for plane-strain extrusion through an eccentric hole and unsymmetrical multi-hole dies. They have validated upper bound results with the published works from the literature and with the finite element method results. The survey of the literature reveals that a simplified analysis of the extrusion through the holes in a square die is not available in the literature.

2. Estimation of ram force by upper bound method

The estimation of ram force is important for the design of the extrusion machine. The upper bound method provides a conservative, i.e., the upper estimate of the ram force. However, finding out an upper bound solution for multi-hole extrusion is complicated. Experimental investigations by Aggarwal et al. [14] reveal that the power required for the multi-hole extrusion is always lower than that for single-hole extrusion, for the same sizes of the holes. Thus, in the present work, power calculation has been carried out based on a single-hole extrusion process. This is a conservative and simplified approach.

* Corresponding author. Tel.: +91 361 2582657 (office), +91 361 2584657/2691036 (residence), +91 9954498115 (mobile); fax: +91 361 2582699.
E-mail addresses: uday@iitg.ernet.in, usd1008@yahoo.com (U.S. Dixit).

0261-3069/$ - see front matter © 2008 Elsevier Ltd. All rights reserved.
doi:10.1016/j.matdes.2008.04.062

The previous studies on the multi-hole extrusion have indicated the presence of dead metal zones in the die [6,12,13]. Here, it is assumed that the flow of the metal through a square die having a single-hole may be considered as the flow through a conical die as shown in Fig. 1. The boundary of the dead metal zone acts like an inner surface of the conical die. The die semi-angle is obtained by minimizing the total power. For the calculation of the power through the conical die, the upper bound model of Reddy et al. [15] has been adopted with a modification to include the effect of bending of the material of the billet at the entry and the exit.

Taking line 1–2 (Fig. 1) and the axis of symmetry as the two stream lines and assuming that all the stream lines are straight, the suitable assumed velocity field is

$$V_z = \frac{V_1 R_1^2}{R^2}, \tag{1}$$

$$V_r = -\frac{V_1 R_1^2 r}{R^3}\tan\alpha, \tag{2}$$

where V_1 is the ram velocity, R_1 is the radius of the billet, R_2 is the radius of extruded product, α is the die semi-angle, and R is the radius of the cone at location z, the r–z coordinate system being shown in Fig. 2. The power of deformation in the assumed conical portion is given by

$$\dot{W}_d = \dot{W}_i + \dot{W}_f + \dot{W}_s, \tag{3}$$

where $\dot{W}_i$ is the internal power of deformation in the conical zone having continuous velocity, $\dot{W}_f$ is the friction power and $\dot{W}_s$ is the power loss due to velocity discontinuities at Sections 1-1 and 2-2 shown in Fig. 1.

The internal power of deformation in the continuous velocity zone is given by

$$\dot{W}_i = \int_0^L \int_0^R \sigma_y \dot{\varepsilon}_{eq} 2\pi r \mathrm{d}r\mathrm{d}z, \tag{4}$$

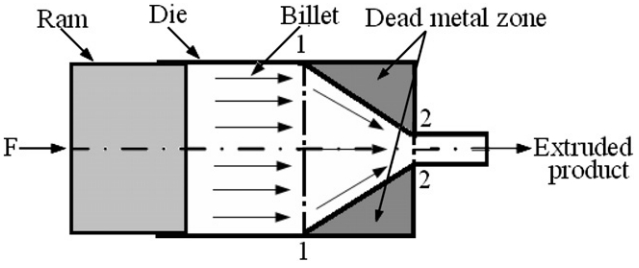

Fig. 1. Schematic diagram of flow of the metal through a square die.

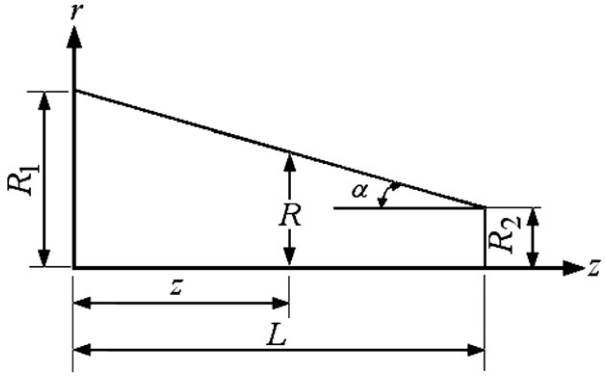

Fig. 2. Enlarged view of the upper half of the conical portion.

where σ_y is the flow stress of the material, $\dot{\varepsilon}_{eq}$ is the equivalent strain-rate, and L is the length of the conical die. Further

$$\dot{\varepsilon}_{eq} = \sqrt{\frac{2}{3}(\dot{\varepsilon}_{rr}^2 + \dot{\varepsilon}_{\theta\theta}^2 + \dot{\varepsilon}_{zz}^2 + 2\dot{\varepsilon}_{rz}^2)}, \tag{5}$$

where

$$\dot{\varepsilon}_{rr} = \frac{\partial V_r}{\partial r}; \quad \dot{\varepsilon}_{\theta\theta} = \frac{V_r}{r}; \quad \dot{\varepsilon}_{zz} = \frac{\partial V_z}{\partial z}; \quad \dot{\varepsilon}_{rz} = \frac{1}{2}\left(\frac{\partial V_r}{\partial z} + \frac{\partial V_z}{\partial_r}\right). \tag{6}$$

For a strain-hardening material, the flow stress may be assumed to be related to strain in the following manner:

$$\sigma_y = K\varepsilon_{eq}^n, \tag{7}$$

where K is the strength coefficient of the material, n is the strain-hardening exponent, and ε_{eq} is the equivalent strain defined by

$$\varepsilon_{eq} = (\varepsilon_{eq})_i + \int_0^t \dot{\varepsilon}_{eq}\mathrm{d}t, \tag{8}$$

where $(\varepsilon_{eq})_i$ the initial equivalent strain due to bending of material at the die inlet and t is the time. The initial equivalent strain is calculated by the following expression [16]:

$$(\varepsilon_{eq})_i = \frac{2}{\sqrt{3}}\tan\left[\frac{1}{2}\tan^{-1}\left(\frac{r}{R}\tan\alpha\right)\right]. \tag{9}$$

Knowing that along a stream-line

$$\mathrm{d}t = \frac{\mathrm{d}z}{V_z} = \frac{\mathrm{d}r}{V_r}. \tag{10}$$

Eq. (8) can be written as

$$\varepsilon_{eq} = \frac{2}{\sqrt{3}}\left[\tan\left\{\frac{1}{2}\tan^{-1}\left(\frac{r}{R}\tan\alpha\right)\right\} + \left\{\sqrt{3 + 2.25\frac{r^4}{R^4}\tan^2\alpha}\right\}\ln\frac{R_1}{R}\right]. \tag{11}$$

The internal power dissipation in the continuous velocity zone is found by numerically integrating Eq. (4).

The frictional power dissipation at the surface of the dead metal zone is given by

$$\dot{W}_f = \int_{R_2}^{R_1} \frac{\sigma_y}{\sqrt{3}}\frac{V_z}{\cos\alpha\sin\alpha}2\pi R\mathrm{d}R. \tag{12}$$

The power dissipation due to velocity discontinuities at Sections 1-1 and 2-2 is given by

$$\dot{W}_s = 2\int_0^{R_1} \frac{\sigma_y}{\sqrt{3}}\frac{2\pi r^2 V_1}{R_1}\tan\alpha\mathrm{d}r. \tag{13}$$

The power dissipation due to friction at the billet–container interface is given by

$$\dot{W}_{Fc} = \frac{m(\sigma_y)_0 2\pi R_1 L_c V_1}{\sqrt{3}}, \tag{14}$$

where $(\sigma_y)_0$ is the yield stress of the material, m is the friction factor at the billet–die interface and L_c is the billet length outside the assumed conical deformation zone.

The total power is given by

$$\dot{W}_t = \dot{W}_d + \dot{W}_{Fc}. \tag{15}$$

The ram force can be obtained by dividing the total power by the ram velocity. The value of the die semi-angle α is obtained by a one-dimensional optimization procedure for minimizing the total power. The average ram pressure is calculated as

$$P_{avg} = \frac{\dot{W}_t}{\pi R_1^2 V_1}. \tag{16}$$

3. Determination of die pressure distribution by using slab method

The estimation of die pressure distribution is important for the design of the die. Slab method is used for the estimation of die pressure distribution in the dead metal zone. Equations of axial and radial equilibrium of a slab are written by assuming that the stresses are uniform over the cross-section. The schematic diagram of axial and radial equilibrium of a typical slab is depicted in Fig. 3. Since the boundary of the dead metal zone acts like the inner surface of the conical die, the friction between the dead metal zone and the flowing material is equal to the shear strength of the material. Thus, in the conical region the value of the friction factor m is taken as 1.

Axial and radial equilibrium of the slab gives

$$R\frac{\mathrm{d}\sigma_{zz}}{\mathrm{d}z} - 2(\sigma_{zz}\tan\alpha + (\sigma_y/\sqrt{3}) + p\tan\alpha) = 0, \tag{17}$$

$$\sigma_{rr} = \frac{\sigma_y}{\sqrt{3}}\tan\alpha - p. \tag{18}$$

Assuming $\sigma_{rr}, \sigma_{\theta\theta}$ and σ_{zz} to be the principal stresses and $\sigma_{rr} = \sigma_{\theta\theta}$, the von-Mises yield condition leads to

$$\sigma_{zz} - \sigma_{rr} = \sigma_y. \tag{19}$$

Eliminating σ_{rr} from Eqs. (18) and (19) leads to

$$p = \frac{\sigma_y}{\sqrt{3}}(\sqrt{3} + \tan\alpha) - \sigma_{zz}. \tag{20}$$

Substituting p from Eq. (20) into Eq. (17) and integrating along the die length, the following expression for σ_{zz} is obtained:

$$\sigma_{zz} = \frac{2}{\sqrt{3}}\int_0^z \sigma_y \left\{\frac{(1+\tan^2\alpha) + \sqrt{3}\tan\alpha}{R}\right\}\mathrm{d}z - P_{\mathrm{avg}}. \tag{21}$$

The values of σ_y and P_{avg} obtained by the upper bound method are used to find σ_{zz} by integrating above equation at any section. Since σ_y varies over the cross-section, the average value is used for a cross-section. The die pressure p at any section is then obtained by putting the value of σ_{zz} in Eq. (20).

4. Design of the ram and the die

The ram is subjected to compressive load and may fail by buckling or compression. The mode of failure of the ram depends upon the slenderness ratio. Slenderness ratio of the ram is defined as the ratio of the length to the least radius of gyration. If the slenderness ratio is high, the ram is considered a column and the failure mode is buckling, whereas if the slenderness ratio is small, the ram is considered a compression member and the failure mode is yielding. For a column, the minimum load at which buckling starts is called the critical load of buckling and is given as [17]

$$F_{\mathrm{cr}} = \frac{n\pi^2 EI}{l^2}, \tag{22}$$

where n is the end-condition constant, E is the modulus of elasticity of the ram material, I is the least moment of inertia about the axis, and l is the length of the ram. For a low slenderness ratio, the ram is designed based upon the compressive strength of the ram material. In general, for steel, if the slenderness ratio is less than 30, the failure occurs due to compression.

The stresses in the die are computed by finite element analysis using the ANSYS package. The contours of the von-Mises stress are plotted. This analysis helps in deciding the wall thickness and the number of holes at the bottom of the die.

5. Observations on the experimental setup

This section describes the test of the materials used in the experiments, the experimental setup and the various other aspects of the experiments. To estimate the mechanical properties of the material used, testing of the material was carried out. Firstly, compression tests were carried out to investigate the hardening behavior of the billet material. Subsequently, tensile test of the die steel (H-13) was carried out to estimate the strength of the die steel. The extrusion machine setup was fabricated and experiments were carried out to study the process. First, the experiments were carried out using a single-hole die with various billet lengths to estimate the friction factor at the die–billet interface. Afterwards, the experiments on multi-hole extrusion process were carried out to investigate the variation of the ram force.

In the present model, lead metal alloy has been used as the billet material. In order to characterize the hardening behavior of the lead metal alloy, compression tests were carried out in a universal testing machine (Instron 8801). A cylindrical specimen of diameter 15 mm and length 30 mm was used for the compression test. To reduce the influence of friction, the specimens were lubricated. The yield strength of the lead metal alloy was found to be 30 MPa. Following relation was fitted for the hardening behavior:

$$\sigma_y = 54.59(\varepsilon_{\mathrm{eq}})^{0.14}\ \mathrm{MPa}. \tag{23}$$

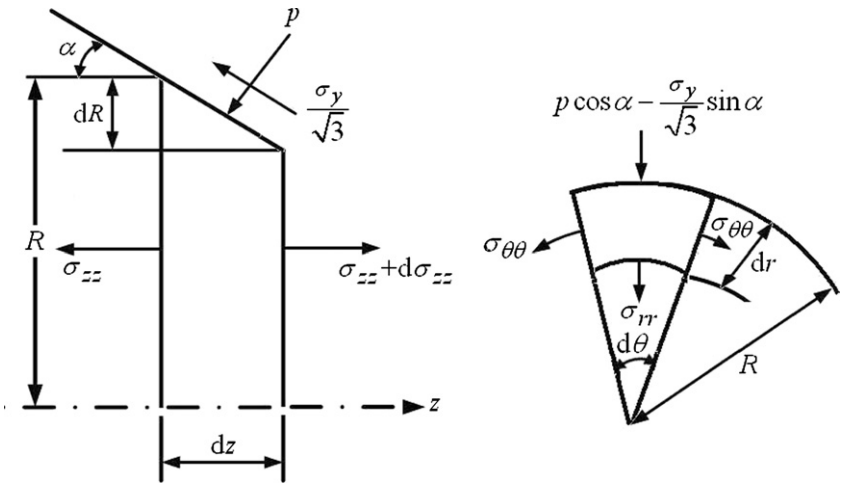

Fig. 3. Axial and radial equilibrium of a slab.

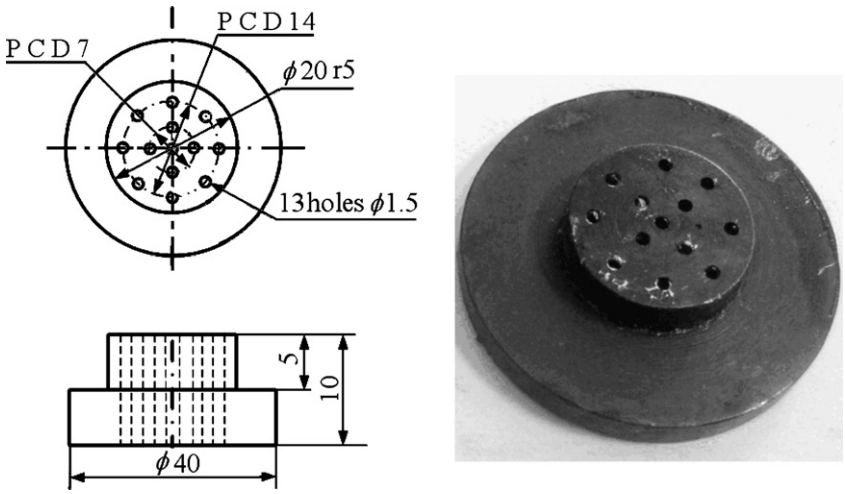

Fig. 4. The bottom piece of the multi-hole extrusion die.

The material used for fabricating the die, the ram and the base plate is die steel (H-13). Tensile test of the die steel specimen was carried out. The yield strength of the die steel was found to be 700 MPa and the ultimate strength 1050 MPa.

The die is in the form of a hollow cylinder of outer diameter 40 mm and inner diameter 20 mm, in which a bottom piece having the holes is inserted. The bottom piece having 13 holes is shown in Fig. 4. In this figure, all dimensions are in mm.

5.1. Comparison between analytical and experimental ram forces

Experiments have been carried out using the billet of lengths 30, 25 and 20 mm using the single-hole die. The ram force–displacement curves obtained in single-hole extrusion are shown with billets of varying lengths in Fig. 5. The value of the friction factor was calculated using the method suggested by Jooybari [18]. According to this method, the friction factor m is given by

$$m = \frac{\sqrt{3}}{2\pi(\sigma_y)_0 R_1}\frac{dF}{dL_c}, \tag{24}$$

where F is the ram force. In the present analysis, the value of the friction factor was found to be 0.63. This calculated value of the friction factor has been used in all other calculations.

Fig. 6 shows the plot between ram force and ram displacement through the multi-hole die for billets of lengths 30, 25 and 20 mm. The diameter of the billet was 20 mm and the extruded wire diameter was 1.5 mm. The ram force for the same billet length is found to be less in the case of the multi-hole extrusion than in the case of the single-hole extrusion. This observation is in agreement with the observation of Aggarwal et al. [14].

Analytical formulae have been developed to calculate the total extrusion power through the single-hole die as discussed in Section 2. Table 1 contains the comparison of analytical and experimental ram forces for different billet lengths in single as well as multi-hole extrusions. It is observed that the analytical results of the single-hole extrusion are about 25% greater than the experimental results. The ram force for the multi-hole extrusion process is about 50% less than for the single-hole extrusion process. Thus, the analytical method presented in this paper provides a conservative estimate of the ram force.

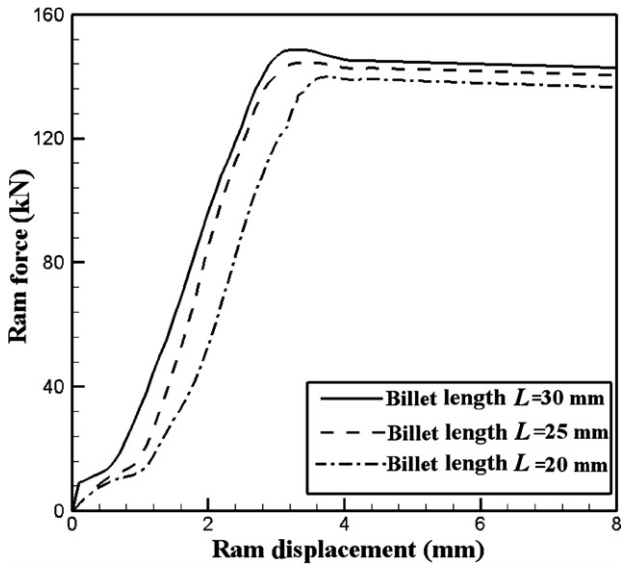

Fig. 5. Experimental ram force–displacement curve in single-hole extrusion.

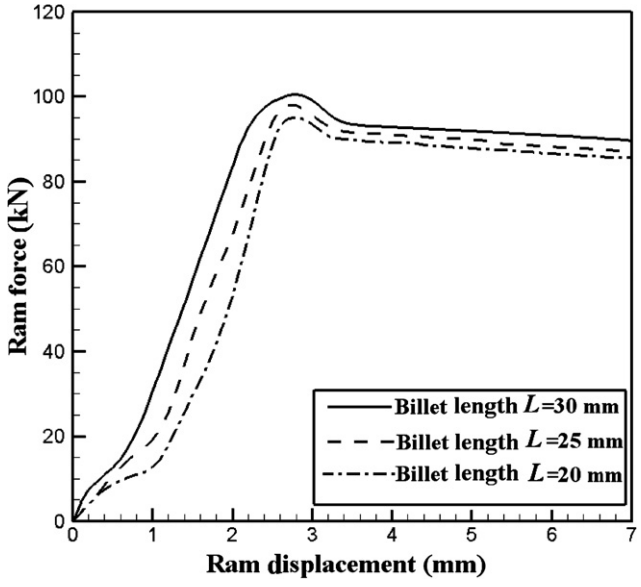

Fig. 6. Experimental ram force–displacement curve in multi-hole extrusion.

Table 1
Comparison between experimental and analytical ram force

Billet length (mm)	Ram force (kN)		
	Analytical	Experimental	
	(single-hole)	Single-hole	Multi-hole
30	186.31	147.97	100.72
25	182.88	144.55	98.7
20	179.45	140.95	95.3

5.2. The lengths of the extruded wires from different holes of the die

It is experimentally observed that the length of the extruded wire is the shortest at the center and is the longest at the holes on a pitch circle diameter of 14 mm. The typical ratio among the lengths of the extruded wires from the central to the outer layers of the holes is 1:2.5:5.5. This may be attributed to the fact that for the outer layer of the holes, the friction factor is less as compared to the friction factor of the central hole. For the outer layer of holes, friction occurs due to the sliding of the billet material over the die surface, whereas for the inner hole, friction is between the different layers of the billet material itself. The friction factor between the different layers of material is 1.

6. Conclusions

In this paper, a methodology for the preliminary design of the multi-hole extrusion process is presented. The estimation of the ram force is carried out using upper bound method by considering the process as a single-hole extrusion. This leads to an overestimation of the ram force, which results in a safer design of the die and ram. Die pressure distribution along the die face has been calculated using the slab method. A finite element analysis of the die has been carried out to estimate the distribution of the von-Mises stresses across the die volume. The experimental investigations have been carried out by extruding the billets made of lead through single-hole and multi-hole dies. The experimental results are compared with the analytical results. To carry out the analysis, the value of the friction factor is found experimentally. It is observed that the ram force calculated by the proposed methodology is about 25% greater than the experimental force for a single-hole extrusion. It is found experimentally that the material encounters more resistance to flow in the central hole than in the holes away from the center. This leads to differences in the lengths of the extruded wires, if the hole-sizes are same. In the case of the multi-hole extrusion, ram force is always lesser (about two-third) than in the case of the single-hole extrusion. Thus, the multi-hole extrusion process can become a productive process for the mass production of small sized components.

References

[1] Iwata K, Osakada K, Fujino S. Analysis of hydrostatic extrusion by the finite element method. Trans ASME J Eng Ind 1972;94:697–703.
[2] Zienkiewicz OC, Jain PC, Onate E. Flow of solids during forming and extrusion: some aspects of numerical solutions. Int J Solids Struct 1978;14:15–38.
[3] Kobayashi S, Oh SI, Altan T. Metal forming and the finite element method. New York: Oxford University Press; 1989.
[4] Balaji PA, Sundararajan T, Lal GK. Viscoplastic deformation analysis and extrusion die design by FEM. Trans ASME J Appl Mech 1991;58:644–50.
[5] Reddy NV, Dixit PM, Lal GK. Central bursting and optimal die profile for axisymmetric extrusion. Trans ASME J Manuf Sci Eng 1996;118:579–84.
[6] Peng Z, Sheppard T. Simulation of multi-hole die extrusion. Mater Sci Eng 2004;367:329–42.
[7] Jooybari MB, Saboori M, Azad MN, Hosseinipour SJ. Combined upper bound and slab method, finite element and experimental study of optimal die profile in extrusion. Mater Des 2007;28:1812–8.
[8] Kumar S, Vijay P. Die design and experiments for shaped extrusion under cold and hot condition. J Mater Process Technol 1999;190:375–81.
[9] Dodeja LC, Johnson W. The cold extrusion of circular rods through square multiple hole dies. J Mech Phys Solids 1957;5:281–95.
[10] Johnson W, Mellor PB, Woo DM. Extrusion through single-hole staggered and unequal multi-hole dies. J Mech Phys Solids 1958;6:203–22.
[11] Keife H. Extrusion through two die openings: a 2D upper-bound analysis checked by plasticine experiments. J Mater Process Technol 1993;37:189–202.
[12] Xie JX, Murakami T, Ikeda K, Takahashi H. Experimental simulation of metal flow in porthole-die extrusion. J Mater Process Technol 1995;49:1–11.
[13] Ulysse P, Johnson RE. A study of the effect of the process variables in unsymmetrical single-hole and multi-hole extrusion processes. J Mater Process Technol 1998;73:213–25.
[14] Aggarwal K, Gupta R, Yaramshetti V. A study of multi-hole extrusion process. B.Tech. Project Report, Department of Mechanical Engineering, IIT Guwahati; 2007.
[15] Reddy NV, Dixit PM, Lal GK. Die design for axisymmetric extrusion. J Mater Process Technol 1995;55:331–9.
[16] Iwahashi Y, Wang J, Hortia Z, Nemoto M, Langdon TG. Principle of equal-channel angular pressing for the processing of ultra-fine grained materials. Scripta Mater 1996;35:143–6.
[17] Shigley JE. Mechanical engineering design. Singapore: McGraw-Hill Book Company; 1986.
[18] Jooybari MB. A theoretical and experimental study of friction in metal forming by the use of the forward extrusion process. J Mater Process Technol 2002;125–126:369–74.